Letter

Search for $K^0_{S(L)} \to \mu^+\mu^-\mu^+\mu^-$ decays at LHCb

R. Aaij *et al.*[*]
(LHCb Collaboration)

(Received 22 December 2022; accepted 23 January 2023; published 3 August 2023)

A search for $K^0_{S(L)} \to \mu^+\mu^-\mu^+\mu^-$ decays is performed using proton-proton collision data collected by the LHCb experiment at a center-of-mass energy of 13 TeV, corresponding to an integrated luminosity of 5.1 fb^{-1}. No evidence for signal is found. The 90% confidence level upper limits are the first set for both decays and are $\mathcal{B}(K^0_S \to \mu^+\mu^-\mu^+\mu^-) < 5.1 \times 10^{-12}$ and $\mathcal{B}(K^0_L \to \mu^+\mu^-\mu^+\mu^-) < 2.3 \times 10^{-9}$.

DOI: 10.1103/PhysRevD.108.L031102

I. INTRODUCTION

The $K^0_S \to \mu^+\mu^-\mu^+\mu^-$ decay is a flavor-changing neutral current process that has not yet been observed. In the Standard Model (SM), its decay rate is highly suppressed, with an expected branching fraction [1]

$$\mathcal{B}(K^0_S \to \mu^+\mu^-\mu^+\mu^-)_{SM} \sim (1-4) \times 10^{-14}. \quad (1)$$

The related channel $K^0_L \to \mu^+\mu^-\mu^+\mu^-$ is predicted in the SM [1] to occur at a higher rate

$$\mathcal{B}(K^0_L \to \mu^+\mu^-\mu^+\mu^-)_{SM} \sim (4-9) \times 10^{-13}. \quad (2)$$

However, since the expected LHCb acceptance for K^0_L decays is $\sim 2 \times 10^{-3}$ times smaller than the K^0_S one [2], the SM $K^0_L \to \mu^+\mu^-\mu^+\mu^-$ yield expected in the experiment is small compared to that of the K^0_S decay.

Physics beyond the SM (BSM) can lead to large enhancements of $\mathcal{B}(K^0_S \to \mu^+\mu^-\mu^+\mu^-)$ with respect to the SM prediction. For instance, proposed dark-sector scenarios can enhance the branching fractions by up to $\sim 2 \times 10^{-12}$ [3,4]. To date, no direct experimental search of these decays has been performed. This paper focuses primarily on a search for the $K^0_S \to \mu^+\mu^-\mu^+\mu^-$ decay, but results for both the $K^0_S \to \mu^+\mu^-\mu^+\mu^-$ and $K^0_L \to \mu^+\mu^-\mu^+\mu^-$ decays are presented.

In this analysis, proton-proton (pp) collision data collected by the LHCb experiment during 2016–2018 at a center-of-mass energy of 13 TeV, corresponding to an integrated luminosity of 5.1 fb^{-1}, are used. The data analysis largely follows the strategy of the $K^0_S \to \mu^+\mu^-$ analyses by the LHCb Collaboration [5,6]. Following those, $\mathcal{B}(K^0_S \to \mu^+\mu^-\mu^+\mu^-)$ and $\mathcal{B}(K^0_L \to \mu^+\mu^-\mu^+\mu^-)$ are measured relative to $\mathcal{B}(K^0_S \to \pi^+\pi^-)$.

II. LHCb DETECTOR AND TRIGGER

The LHCb detector [7,8] is a single-arm forward spectrometer covering the pseudorapidity range $2 < \eta < 5$, designed for the study of particles containing b or c quarks. The detector includes a high-precision tracking system consisting of a silicon-strip vertex detector (VELO) surrounding the pp interaction region [9], a large-area silicon-strip detector located upstream of a dipole magnet with a bending power of about 4 Tm, and three stations of silicon-strip detectors and straw drift tubes [10] placed downstream of the magnet. The tracking system provides a measurement of the momentum, p, of charged particles with a relative uncertainty that varies from 0.5% at low momentum to 1.0% at 200 GeV/c. The minimum distance of a track to a proton-proton collision vertex (PV), the impact parameter (IP), is measured with a resolution of $(15 + 29/p_T)$ μm, where p_T is the component of the momentum transverse to the beam axis, in GeV/c. Different types of charged hadrons are distinguished using information from two ring-imaging Cherenkov (RICH) detectors [11]. Photons, electrons and hadrons are identified by a calorimeter system consisting of a scintillating pad and preshower detectors, an electromagnetic and a hadronic calorimeter. Muons are identified by a system composed of alternating layers of iron and multiwire proportional chambers [12]. In addition, information from the tracking system, the calorimeter system and the RICH detectors is used to further improve the muon identification. The LHCb detector accumulated data in two data-taking periods; Run 1 (2011–2012) and Run 2 (2015–2018).

Events are first filtered by a hardware trigger, known as L0 [13], which uses information from the calorimeter and the muon system to select p_T signatures above a few

[*]Full author list given at the end of the article.

GeV/c. Subsequently, a full event reconstruction is applied in the high-level trigger (HLT), which runs in two separate steps (HLT1 and HLT2). In analyses of kaon decays to muons using data recorded prior to 2016, the search was limited by a requirement of at least one muon with p_{T} above 1.8 GeV/c at HLT1. In 2016, a new reconstruction algorithm allowed the muon p_{T} threshold requirement in the HLT to be reduced to 80 MeV/c [14]. In addition, a dedicated set of software trigger selections was developed for the HLT1 stage [15]. This increased the trigger efficiency for selecting strange hadrons decaying into muons by an order of magnitude with respect to the LHCb Run 1 data sample [15].

Given its large branching fraction [16], the $K^0_{\mathrm{S}} \to \pi^+\pi^-$ decay is used as the normalization mode in this search. The use of this normalization mode cancels part of the systematic uncertainties from signal detection efficiency, and does not require knowledge of the absolute kaon production cross section and integrated luminosity. The $K^0_{\mathrm{S}} \to \pi^+\pi^-$ candidates are reconstructed from trigger-unbiased data selected by a quasirandom trigger with minimal requirements ensuring some event activity. The K^0_{S} candidates from both the signal and the normalization channel are required to come from the PV. Simulation is used to model the effects of the detector acceptance and selection requirements. In the simulation, pp collisions are generated using PYTHIA 8 [17,18] with a specific LHCb configuration [19]. Decays of unstable particles are described by EvtGen [20], in which final-state radiation is generated using PHOTOS [21]. The interaction of the generated particles with the detector, and its response, are implemented using the Geant4 toolkit [22,23] as described in Ref. [24].

III. STRATEGY

This measurement benefits from both the large prompt K^0_{S} and K^0_{L} production cross sections at the LHC (with cross sections times multiplicity of order 0.3 barn each [2]), as well as the forward production of kaons which fall within the LHCb detector acceptance. Candidates of $K^0_{\mathrm{S}} \to \mu^+\mu^-\mu^+\mu^-$ decays are reconstructed from two pairs of muons with opposite charges, forming a sufficiently detached secondary vertex with an invariant mass lower than 600 MeV/c^2. A blinding procedure is followed. Selected candidates in the four-muon invariant-mass region 490 MeV/$c^2 < m_{4\mu} <$ 510 MeV/c^2, which, estimated from simulation, contains ≈97% of the signal, are removed from the data sample until the analysis procedure is finalized. The four-muon mass resolution is approximately 4 MeV/c^2.

The data sample is split according to the L0 hardware trigger decision; a category where an object in the event other than the muons from the $K^0_{\mathrm{S}} \to \mu^+\mu^-\mu^+\mu^-$ candidate fires L0 (triggered independently of signal, TIS), and a category where the muons from $K^0_{\mathrm{S}} \to \mu^+\mu^-\mu^+\mu^-$ candidates satisfy muon-related L0 requirements (exclusively triggered on signal, xTOS) [25]. At the HLT stage, the trigger decision must be caused by one of the signal muon candidates. The analysis is performed separately on two independent datasets, labeled TIS and xTOS in reference to the L0 decision, hereafter referred to as trigger categories. Each category comprises roughly 50% of the signal candidates. Since decays occurring inside the VELO can be reconstructed with better invariant-mass resolution than decays outside the VELO, and because the trigger relies on tracks with hits within the VELO and downstream tracking stations, only decays occurring inside the VELO are considered in this analysis. The LHCb decay-time acceptance is such that it makes $K^0_{\mathrm{L}} \to \mu^+\mu^-\mu^+\mu^-$ and $K^0_{\mathrm{S}} \to \mu^+\mu^-\mu^+\mu^-$ decays difficult to differentiate [2]. For this reason, $K^0_{\mathrm{L}} \to \mu^+\mu^-\mu^+\mu^-$ decays are neglected when setting an upper limit on $\mathcal{B}(K^0_{\mathrm{S}} \to \mu^+\mu^-\mu^+\mu^-)$ and vice versa. This approach yields conservative upper limits in the presence of signal. If a signal were to be observed, it would be identified as $K^0_{\mathrm{S(L)}} \to \mu^+\mu^-\mu^+\mu^-$, without specifying the K^0 mass eigenstate.

IV. SIGNAL SELECTION

Several selection requirements are applied to the signal candidate events to further reduce background contributions. These include requirements on the track quality, track χ^2_{IP} (defined as the difference in the vertex-fit χ^2 of a given PV reconstructed with and without the track being considered), and particle identification (PID) of the muons. The $K^0_{\mathrm{S}} \to \pi^+\pi^-$ candidates are also selected using track quality, χ^2_{IP}, and PID requirements, in addition to a requirement on the variables from the Armenteros-Podolanski plane [26] to reduce contributions from $\Lambda \to p\pi^-$ decays.

The dominant background source in the signal channel arises from random combinations of tracks originating near a pp interaction region or from inelastic interactions with the detector material. Potential peaking background contributions from $K^0 \to \pi^+\pi^-\mu^+\mu^-$, $K^0 \to \mu^+\mu^-e^+e^-$, and $K^0 \to \pi^+\pi^-e^+e^-$ decays are studied using simulation and are found to be negligible. A boosted decision tree (BDT) [27,28] classifier implemented in the TMVA toolkit [29,30] is used to further separate signal from combinatorial background. One BDT per trigger category (TIS and xTOS) is trained. The discriminating variables included in the BDTs are

(i) the significance of the distance from the candidate decay vertex to any VELO element or the RF-foil [31], to eliminate background from material interactions;
(ii) the smallest IP of each of the four muon candidates with respect to any of the PVs reconstructed in the event, to eliminate background from final state tracks originating close to the pp interaction point;

(iii) the smallest IP of the K^0_S candidates to any of the PVs reconstructed in the event, to discriminate against background that does not point to a primary vertex;
(iv) the transverse displacement of the K^0_S candidate decay vertex from the beam line, to eliminate background from tracks close to the pp interaction point;
(v) the maximum distance of closest approach between the four final-state tracks, which is expected to be larger for background from random combinations of tracks; and
(vi) and the minimum angle between each pair of muons, which significantly reduces background contributions with at least two VELO tracks sharing hits.

The BDT is trained with simulated $K^0_S \to \mu^+\mu^-\mu^+\mu^-$ decays as a proxy for signal, and $K^0_S \to \mu^+\mu^-\mu^+\mu^-$ candidates from the invariant-mass sidebands in data, which cover $450\ \mathrm{MeV}/c^2 < m_{4\mu} < 490\ \mathrm{MeV}/c^2$ and $510\ \mathrm{MeV}/c^2 < m_{4\mu} < 600\ \mathrm{MeV}/c^2$, as a proxy for background. The samples are randomly split into two subsamples for cross-validation [32], to ensure that the BDT applied to a candidate is always trained on events that are independent of the candidate.

The BDT requirement is optimized for the best expected limit at a 90% confidence level using simulated pseudoexperiments. The signal efficiency of the BDT requirement is approximately 80% while retaining less than one per mille of the background candidates. After the BDT selection requirement, in the case of multiple candidates per event, a single candidate, randomly chosen, is retained.

V. NORMALIZATION AND INVARIANT-MASS FIT

The signal yield, $N_{K^0_S\to\mu^+\mu^-\mu^+\mu^-}$, is translated to a branching fraction via a normalization to $K^0_S \to \pi^+\pi^-$ decays, as

$$\mathcal{B}(K^0_S \to \mu^+\mu^-\mu^+\mu^-) \equiv \alpha N_{K^0_S\to\mu^+\mu^-\mu^+\mu^-}. \quad (3)$$

The normalization factor α, or single event sensitivity,[1] is calculated as

$$\alpha = \mathcal{B}(K^0_S \to \pi^+\pi^-) \times \frac{\varepsilon_{K^0_S\to\pi^+\pi^-} \times s_{\mathrm{MB}}}{N^{\mathrm{MB}}_{K^0_S\to\pi^+\pi^-} \times \varepsilon_{K^0_S\to\mu^+\mu^-\mu^+\mu^-}}, \quad (4)$$

where $\varepsilon_{K^0_S\to\pi^+\pi^-}(\varepsilon_{K^0_S\to\mu^+\mu^-\mu^+\mu^-})$ represents the product of the reconstruction, trigger and selection efficiency of $K^0_S \to \pi^+\pi^-$ ($K^0_S \to \mu^+\mu^-\mu^+\mu^-$) candidates. The observed number of $K^0_S \to \pi^+\pi^-$ decays is $N^{\mathrm{MB}}_{K^0_S\to\pi^+\pi^-}$, $\mathcal{B}(K^0_S \to \pi^+\pi^-)$ is the branching fraction of the normalization channel, fixed to $(69.20 \pm 0.05)\%$ [16], and s_{MB} is the prescale factor of the minimum bias trigger averaged over the different data files weighted by integrated luminosity.

[1]The value of $\mathcal{B}(K^0_S \to \mu^+\mu^-\mu^+\mu^-)$ corresponding to one signal event seen in the data sample.

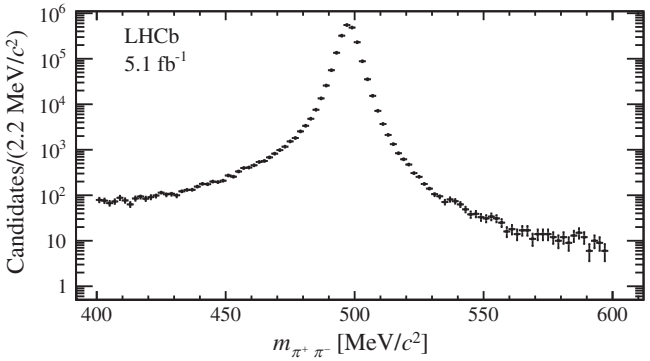

FIG. 1. Invariant-mass distribution for the $K^0_S \to \pi^+\pi^-$ selected candidates in the full dataset. The background level is estimated to be at the 1% level or below.

The observed number of $K^0_S \to \pi^+\pi^-$ decays, $N^{\mathrm{MB}}_{K^0_S\to\pi^+\pi^-}$, is estimated as the number of candidates in the mass range $400 < m_{\pi^+\pi^-} < 600\ \mathrm{MeV}/c^2$, without a fit to the invariant-mass distribution. The background is neglected due to the high purity obtained after applying the same track quality requirements as in the signal channel, as well as requirements on the transverse displacement of the K^0_S decay vertex from the beam line and the distance of the K^0_S decay vertex from any detector material. Figure 1 shows the invariant-mass distribution of the $K^0_S \to \pi^+\pi^-$ candidates satisfying these requirements.

The efficiencies are factorized as

$$\varepsilon = \varepsilon^{\mathrm{REC}}\varepsilon^{\mathrm{SEL/REC}}\varepsilon^{\mathrm{TRIG/SEL}}, \quad (5)$$

where $\varepsilon^{\mathrm{REC}}$ is the reconstruction efficiency (∼0.4% for $K^0_S \to \mu^+\mu^-\mu^+\mu^-$ decays) including acceptance effects, $\varepsilon^{\mathrm{SEL/REC}}$ is the efficiency of selecting the reconstructed signal candidates, including the BDT and PID cuts (∼38% for $K^0_S \to \mu^+\mu^-\mu^+\mu^-$ decays) and $\varepsilon^{\mathrm{TRIG/SEL}}$ is the trigger efficiency for events that would have been otherwise selected for offline analysis (∼20% for $K^0_S \to \mu^+\mu^-\mu^+\mu^-$ decays). The efficiencies are calculated using simulated events with corrections derived from $K^0_S \to \pi^+\pi^-$ decays in data. Tracking efficiencies are obtained from $J/\psi \to \mu^+\mu^-$ in data and $K^0_S \to \pi^+\pi^-$ decays using a tag-and-probe method [33].

Similarly, PID efficiencies are obtained using calibration samples of low-momentum muons from $J/\psi \to \mu^+\mu^-$ decays collected at the same time as the data used for the analysis, and divided into six samples according to different data-taking conditions. The trigger efficiencies obtained in simulation are validated with misidentified $K^0 \to \pi^\pm\mu^\mp\overset{(-)}{\nu}_\mu$ decays, as done in Ref. [34].

The signal yield $N_{K^0_S\to\mu^+\mu^-\mu^+\mu^-}$ is obtained from a maximum-likelihood fit to the four-muon invariant-mass distributions of the signal candidates in the two trigger categories. The invariant-mass distributions of background

events in the signal channel is assumed to be an exponential function. This assumption is validated using background events with lower values of the BDT output. The $K^0_S \to \mu^+\mu^-\mu^+\mu^-$ signal invariant-mass shape is parameterized using a Hypatia distribution [35]. The parameter values of the signal distribution are obtained from simulated events with corrections obtained from $K^0_S \to \pi^+\pi^-$ decays in data, following Ref. [34].

VI. SYSTEMATIC UNCERTAINTIES

The systematic uncertainties are incorporated as Gaussian constraints to the fit of the signal-candidate mass distribution. For convenience, systematic sources are separated into those acting independently on each trigger category and those affecting the overall normalization. Table I shows the main systematic uncertainties determined for this analysis. The different sources of systematic uncertainties are summarized as follows:

(i) The uncertainty on the branching fraction $\mathcal{B}(K^0_S \to \pi^+\pi^-) = (69.20 \pm 0.05)\%$ induces a 0.07% uncertainty on the normalization.

(ii) The uncertainty on the average minimum bias prescale factor $s_{\rm MB}$ is 0.3%.

(iii) A 1% systematic accounts for small changes throughout the Run 2 data taking. These are mostly due to changes in the trigger settings, and were determined by comparing the yields of misidentified triggered $K^0 \to \pi^\pm\mu^\mp\overset{(-)}{\nu}_\mu$ decays with $K^0_S \to \pi^+\pi^-$ decays from the minimum bias data.

(iv) To account for residual differences between data and simulation, the efficiency ratio is recomputed with and without simulation corrections to the kaon momenta and track quality parameters. Half of the correction is taken as a systematic uncertainty (4.4%).

(v) The systematic uncertainty on the $K^0_S \to \pi^+\pi^-$ yield is evaluated by comparing the yield obtained from a fit to the $\pi^+\pi^-$ invariant mass with floating background components, with the default yield, which neglects the background contribution since the sample has very high purity. This effect is found to be less than 1%.

(vi) The uncertainty is assigned as the difference between the maximum and minimum values of the six correction factors for the PID mentioned above.

(vii) A systematic uncertainty associated to differences between data and simulation in the track reconstruction efficiency is determined using control channels from data.

(viii) Potential differences in the trigger efficiencies between data and simulation are a source for systematic uncertainties. The L0 and HLT efficiencies for the $K^0_S \to \mu^+\mu^-\mu^+\mu^-$ signal are determined using misidentified $K^0 \to \pi^\pm\overset{(-)}{\nu}$ decays as control modes. The efficiencies are found to be compatible between data and simulation, and the uncertainty in the validation is used as the systematic uncertainty, following Ref. [36]. The $K^0 \to \pi^\pm\mu^\mp\overset{(-)}{\nu}$ sample at LHCb is composed of K^0_S and K^0_L in similar amounts, due to a compensation between the different branching fractions [37–39], and the different reconstruction efficiency caused by the decay-time acceptance. The decay-time acceptance also results in similar decay-time distributions for the reconstructed K^0_L and K^0_S decays.

In addition, a systematic uncertainty of 1.4% is added to the relative efficiency between $K^0_S \to \mu^+\mu^-\mu^+\mu^-$ and $K^0_L \to \mu^+\mu^-\mu^+\mu^-$ decays, when measuring $\mathcal{B}(K^0_L \to \mu^+\mu^-\mu^+\mu^-)$. This systematic uncertainty covers the difference of the efficiency ratio across the data-taking period as well as the uncertainties from the simulated sample size. The systematic uncertainties from signal and background invariant-mass models are negligible for the current level of precision.

TABLE I. Summary of systematic uncertainties.

Source	Relative effect (%)
$\mathcal{B}(K^0_S \to \pi^+\pi^-)$	0.07
$s_{\rm MB}$	0.30
Variations in data taking	1
Data/simulation differences	4.40
$K^0_S \to \pi^+\pi^-$ yield	1
PID	3.30
Tracking	1.20
$\varepsilon^{\rm L0}$	10 (TIS), 21 (xTOS)
$\varepsilon^{\rm HLT/L0}$	11
Total	16 (TIS), 24 (xTOS)

VII. RESULTS

The number of $K^0_S \to \pi^+\pi^-$ decays in the dataset corrected by the s_{MB} prescale factor is $(3.96 \pm 0.04) \times 10^{12}$. The efficiency ratio $\varepsilon_{K^0_S\to\pi^+\pi^-}/\varepsilon_{K^0_S\to\mu^+\mu^-\mu^+\mu^-}$ is 27.0 ± 4.3 (21.6 ± 5.3) for the TIS (xTOS) category. The obtained normalization factors are $\alpha_{\rm TIS} = (4.7 \pm 0.8) \times 10^{-12}$ and $\alpha_{\rm xTOS} = (3.8 \pm 0.9) \times 10^{-12}$. The combined single-event sensitivity is $\alpha \approx 2.10 \times 10^{-12}$. These values assume that the muons are distributed uniformly in phase space for $K^0_S \to \mu^+\mu^-\mu^+\mu^-$ decays. Nevertheless, the efficiency is nearly uniform as a function of the muon helicity angles and for most of the dimuon invariant masses, except near the kinematic thresholds. Thus, the results are valid for a wide range of BSM models unless the dimuons originate from a new resonance with an invariant mass close to half of the K^0_S mass or very close to twice the muon mass. The former strengthens the limit while the latter weakens it. The result also assumes that the muons are produced at the K^0 decay vertex.

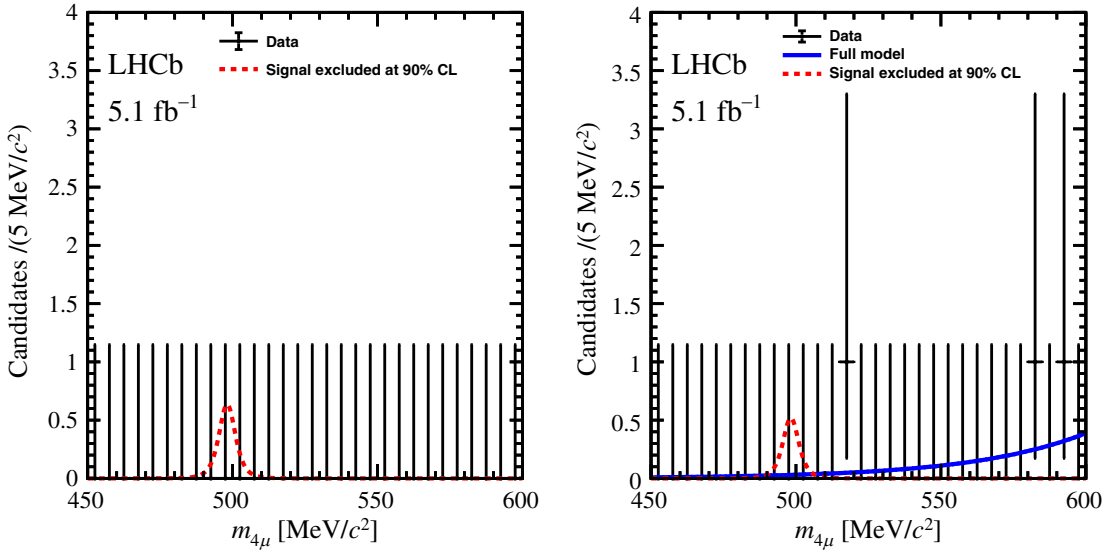

FIG. 2. Invariant-mass distribution of the observed $K^0_S \to \mu^+\mu^-\mu^+\mu^-$ candidates in the (left) xTOS trigger category, and (right) TIS trigger category. The blue lines represent the simultaneous fit to both categories, using the exponential functions to represent the background. The expected $K^0_S \to \mu^+\mu^-\mu^+\mu^-$ signal for the branching fraction excluded at 90% CL is shown with a dotted red line.

The invariant-mass distributions of the selected candidate events are shown in Fig. 2. No events are observed in the signal mass window 490–510 MeV/c^2, for both the xTOS and TIS samples. Integrating the profile likelihood from the positive side of the branching fraction, the upper limits at 90% CL are found to be

$$\mathcal{B}(K^0_S \to \mu^+\mu^-\mu^+\mu^-) < 5.1 \times 10^{-12},$$
$$\mathcal{B}(K^0_L \to \mu^+\mu^-\mu^+\mu^-) < 2.3 \times 10^{-9},$$

which coincide with the upper limits expected in absence of signal.

While the data used to produce the results here were collected using a 1 MHz hardware trigger, the upgraded LHCb detector fully reconstructs events at the LHC inelastic event rate of 30 MHz [40]. This will increase the trigger efficiency of the $K^0_S \to \mu^+\mu^-\mu^+\mu^-$ events by about a factor five [40], giving the possibility to reach sensitivities at the SM level, $\mathcal{B}(K^0_S \to \mu^+\mu^-\mu^+\mu^-) \sim (1-4) \times 10^{-14}$, with 300 fb^{-1} of integrated luminosity.

VIII. CONCLUSIONS

A search for $K^0_{S(L)} \to \mu^+\mu^-\mu^+\mu^-$ has been performed analyzing 5.1 fb^{-1} of LHCb data recorded from 2016 to 2018. No signal is observed. The obtained upper limits are the first reported for the $K^0_{S(L)} \to \mu^+\mu^-\mu^+\mu^-$ decay modes. The observed values are close to the maximum values allowed in the dark photon models [3] and indicate very good prospects for the LHCb upgrade, which could achieve sensitivities at the level of the SM prediction for $\mathcal{B}(K^0_S \to \mu^+\mu^-\mu^+\mu^-)$ using 300 fb^{-1} of integrated luminosity.

ACKNOWLEDGMENTS

We express our gratitude to our colleagues in the CERN accelerator departments for the excellent performance of the LHC. We thank the technical and administrative staff at the LHCb institutes. We acknowledge support from CERN and from the national agencies: CAPES, CNPq, FAPERJ and FINEP (Brazil); MOST and NSFC (China); CNRS/IN2P3 (France); BMBF, DFG and MPG (Germany); INFN (Italy); NWO (Netherlands); MNiSW and NCN (Poland); MEN/IFA (Romania); MICINN (Spain); SNSF and SER (Switzerland); NASU (Ukraine); STFC (United Kingdom); DOE NP and NSF (USA). We acknowledge the computing resources that are provided by CERN, IN2P3 (France), KIT and DESY (Germany), INFN (Italy), SURF (Netherlands), PIC (Spain), GridPP (United Kingdom), CSCS (Switzerland), IFIN-HH (Romania), CBPF (Brazil), Polish WLCG (Poland) and NERSC (USA). We are indebted to the communities behind the multiple open-source software packages on which we depend. Individual groups or members have received support from ARC and ARDC (Australia); Minciencias (Colombia); AvH Foundation (Germany); EPLANET, Marie Skłodowska-Curie Actions and ERC (European Union); A*MIDEX, ANR, IPhU and Labex P2IO, and Région Auvergne-Rhône-Alpes (France); Key Research Program of Frontier Sciences of CAS, CAS PIFI, CAS CCEPP, Fundamental Research Funds for the Central Universities, and Science and Technology Program of Guangzhou (China); GVA, XuntaGal, GENCAT and Prog. Atracción Talento, CM (Spain); SRC (Sweden); the Leverhulme Trust, the Royal Society and UKRI (United Kingdom).

[1] G. D'Ambrosio, D. Greynat, and G. Vulvert, Standard model and new physics contributions to K_L and K_S into four leptons, Eur. Phys. J. C **73**, 2678 (2013).

[2] A. A. Alves Junior *et al.*, Prospects for measurements with strange hadrons at LHCb, J. High Energy Phys. 05 (2019) 048.

[3] E. Goudzovski *et al.*, New physics searches at kaon and hyperon factories, Rep. Prog. Phys. **86**, 016201 (2023).

[4] M. Hostert and M. Pospelov, Novel multilepton signatures of dark sectors in light meson decays, Phys. Rev. D **105**, 015017 (2022).

[5] R. Aaij *et al.* (LHCb Collaboration), Constraints on the $K_S^0 \to \mu^+\mu^-$ Branching Fraction, Phys. Rev. Lett. **125**, 1231801 (2020).

[6] R. Aaij *et al.* (LHCb Collaboration), Search for the rare decay $K_S^0 \to \mu^+\mu^-$, J. High Energy Phys. 01 (2013) 090.

[7] A. A. Alves, Jr. *et al.* (LHCb Collaboration), The LHCb detector at the LHC, J. Instrum. **3**, S08005 (2008).

[8] LHCb Collaboration, LHCb detector performance, Int. J. Mod. Phys. A **30**, 1530022 (2015).

[9] R. Aaij *et al.*, Performance of the LHCb vertex locator, J. Instrum. **9**, P09007 (2014).

[10] P. d'Argent *et al.*, Improved performance of the LHCb outer tracker in LHC run 2, J. Instrum. **9**, P11016 (2017).

[11] M. Adinolfi *et al.*, Performance of the LHCb RICH detector at the LHC, Eur. Phys. J. C **73**, 2431 (2013).

[12] A. A. Alves, Jr. *et al.*, Performance of the LHCb muon system, J. Instrum. **8**, P02022 (2013).

[13] R. Aaij *et al.*, The LHCb trigger and its performance in 2011, J. Instrum. **8**, P04022 (2013).

[14] R. Aaij *et al.*, Optimization of the muon reconstruction algorithms for LHCb run 2, Report No. LHCb-PUB-2017-007, 2017.

[15] F. Dettori, D. Martinez Santos, and J. Prisciandaro, Low-p_T dimuon triggers at LHCb in run 2, Report No. LHCb-PUB-2017-023, 2017.

[16] R. L. Workman *et al.* (Particle Data Group), Review of particle physics, Prog. Theor. Exp. Phys. **2022**, 083C01 (2022).

[17] T. Sjöstrand, S. Mrenna, and P. Skands, A brief introduction to PYTHIA 8.1, Comput. Phys. Commun. **178**, 852 (2008).

[18] T. Sjöstrand, S. Mrenna, and P. Skands, PYTHIA 6.4 physics and manual, J. High Energy Phys. 05 (2006) 026.

[19] I. Belyaev *et al.*, Handling of the generation of primary events in Gauss, the LHCb simulation framework, J. Phys. Conf. Ser. **331**, 032047 (2011).

[20] D. J. Lange, The EvtGen particle decay simulation package, Nucl. Instrum. Methods Phys. Res., Sect. A **462**, 152 (2001).

[21] N. Davidson, T. Przedzinski, and Z. Was, PHOTOS interface in C++: Technical and physics documentation, Comput. Phys. Commun. **199**, 86 (2016).

[22] J. Allison *et al.* (Geant4 Collaboration), Geant4 developments and applications, IEEE Trans. Nucl. Sci. **53**, 270 (2006).

[23] S. Agostinelli *et al.* (Geant4 Collaboration), Geant4: A simulation toolkit, Nucl. Instrum. Methods Phys. Res., Sect. A **506**, 250 (2003).

[24] M. Clemencic, G. Corti, S. Easo, C. R. Jones, S. Miglioranzi, M. Pappagallo, and P. Robbe, The LHCb simulation application, Gauss: Design, evolution and experience, J. Phys. Conf. Ser. **331**, 032023 (2011).

[25] J. A. Hernando Morata *et al.*, Measurement of trigger efficiencies and biases, Reports No. LHCb-2008-073, No. CERN-LHCb-2008-073, CERN, Geneva, 2010.

[26] J. Podolanski and R. Armenteros, Analysis of V-events, Philos. Mag. **45**, 13 (1954).

[27] L. Breiman, J. H. Friedman, R. A. Olshen, and C. J. Stone, *Classification and Regression Trees* (Wadsworth International Group, Belmont, California, USA, 1984).

[28] Y. Freund and R. E. Schapire, A decision-theoretic generalization of on-line learning and an application to boosting, J. Comput. Syst. Sci. **55**, 119 (1997).

[29] H. Voss, A. Hoecker, J. Stelzer, and F. Tegenfeldt, TMVA—Toolkit for multivariate data analysis, Proc. Sci. ACAT2007 (**2007**) 040.

[30] A. Hoecker *et al.*, TMVA 4—Toolkit for multivariate data analysis. Users guide, arXiv:physics/0703039.

[31] M. Alexander *et al.*, Mapping the material in the LHCb vertex locator using secondary hadronic interactions, J. Instrum. **13**, P06008 (2018).

[32] F. Pedregosa *et al.*, SCIKIT-LEARN: Machine learning in Python, J. Mach. Learn. Res. **12**, 2825 (2011), https://www.jmlr.org/papers/volume12/pedregosa11a/pedregosa11a.pdf; see also http://scikit-learn.org.

[33] LHCb Collaboration, Measurement of the track reconstruction efficiency at LHCb, J. Instrum. **10**, P02007 (2015).

[34] R. Aaij *et al.* (LHCb Collaboration), Search for the rare decay $K_S \to \mu^+\mu^-$, J. High Energy Phys. 01 (2013) 090.

[35] D. Martínez Santos and F. Dupertuis, Mass distributions marginalized over per-event errors, Nucl. Instrum. Methods Phys. Res., Sect. A **764**, 150 (2014).

[36] R. Aaij *et al.* (LHCb Collaboration), Constraints on the $K_S^0 \to \mu^+\mu^-$ Branching Fraction, Phys. Rev. Lett. **125**, 231801 (2020).

[37] F. Ambrosino *et al.* (KLOE Collaboration), Measurements of the absolute branching ratios for the dominant K_L decays, the K_L lifetime, and V_{us} with the KLOE detector, Phys. Lett. B **632**, 43 (2006).

[38] F. Ambrosino *et al.* (KLOE Collaboration), Measurement of the K_L meson lifetime with the KLOE detector, Phys. Lett. B **626**, 15 (2005).

[39] D. Babusci *et al.* (KLOE-2 Collaboration), Measurement of the branching fraction for the decay $K_S \to \pi\mu\nu$ with the KLOE detector, Phys. Lett. B **804**, 135378 (2020).

[40] LHCb Collaboration, LHCb upgrade GPU high level trigger technical design report, Report No. CERN-LHCC-2020-006, 2020.

R. Aaij,[32] A. S. W. Abdelmotteleb,[50] C. Abellan Beteta,[44] F. Abudinén,[50] T. Ackernley,[54] B. Adeva,[40] M. Adinolfi,[48] P. Adlarson,[77] H. Afsharnia,[9] C. Agapopoulou,[13] C. A. Aidala,[78] Z. Ajaltouni,[9] S. Akar,[59] K. Akiba,[32] P. Albicocco,[23] J. Albrecht,[15] F. Alessio,[42] M. Alexander,[53] A. Alfonso Albero,[39] Z. Aliouche,[56] P. Alvarez Cartelle,[49] R. Amalric,[13] S. Amato,[2] J. L. Amey,[48] Y. Amhis,[11,42] L. An,[42] L. Anderlini,[22] M. Andersson,[44] A. Andreianov,[38] M. Andreotti,[21] D. Andreou,[62] D. Ao,[6] F. Archilli,[17] A. Artamonov,[38] M. Artuso,[62] E. Aslanides,[10] M. Atzeni,[44] B. Audurier,[12] I. B Bachiller Perea,[8] S. Bachmann,[17] M. Bachmayer,[43] J. J. Back,[50] A. Bailly-reyre,[13] P. Baladron Rodriguez,[40] V. Balagura,[12] W. Baldini,[21,42] J. Baptista de Souza Leite,[1] M. Barbetti,[22,b] R. J. Barlow,[56] S. Barsuk,[11] W. Barter,[52] M. Bartolini,[49] F. Baryshnikov,[38] J. M. Basels,[14] G. Bassi,[29,c] B. Batsukh,[4] A. Battig,[15] A. Bay,[43] A. Beck,[50] M. Becker,[15] F. Bedeschi,[29] I. B. Bediaga,[1] A. Beiter,[62] V. Belavin,[38] S. Belin,[40] V. Bellee,[44] K. Belous,[38] I. Belov,[38] I. Belyaev,[38] G. Benane,[10] G. Bencivenni,[23] E. Ben-Haim,[13] A. Berezhnoy,[38] R. Bernet,[44] S. Bernet Andres,[76] D. Berninghoff,[17] H. C. Bernstein,[62] C. Bertella,[56] A. Bertolin,[28] C. Betancourt,[44] F. Betti,[42] Ia. Bezshyiko,[44] S. Bhasin,[48] J. Bhom,[35] L. Bian,[68] M. S. Bieker,[15] N. V. Biesuz,[21] P. Billoir,[13] A. Biolchini,[32] M. Birch,[55] F. C. R. Bishop,[49] A. Bitadze,[56] A. Bizzeti, M. P. Blago,[49] T. Blake,[50] F. Blanc,[43] J. E. Blank,[15] S. Blusk,[62] D. Bobulska,[53] J. A. Boelhauve,[15] O. Boente Garcia,[12] T. Boettcher,[59] A. Boldyrev,[38] C. S. Bolognani,[74] R. Bolzonella,[21,d] N. Bondar,[38,42] F. Borgato,[28] S. Borghi,[56] M. Borsato,[17] J. T. Borsuk,[35] S. A. Bouchiba,[43] T. J. V. Bowcock,[54] A. Boyer,[42] C. Bozzi,[21] M. J. Bradley,[55] S. Braun,[60] A. Brea Rodriguez,[40] J. Brodzicka,[35] A. Brossa Gonzalo,[40] J. Brown,[54] D. Brundu,[27] A. Buonaura,[44] L. Buonincontri,[28] A. T. Burke,[56] C. Burr,[42] A. Bursche,[66] A. Butkevich,[38] J. S. Butter,[32] J. Buytaert,[42] W. Byczynski,[42] S. Cadeddu,[27] H. Cai,[68] R. Calabrese,[21,d] L. Calefice,[15] S. Cali,[23] M. Calvi,[26,e] M. Calvo Gomez,[76] P. Campana,[23] D. H. Campora Perez,[74] A. F. Campoverde Quezada,[6] S. Capelli,[26,e] L. Capriotti,[20] A. Carbone,[20,f] R. Cardinale,[24,g] A. Cardini,[27] P. Carniti,[26,e] L. Carus,[14] A. Casais Vidal,[40] R. Caspary,[17] G. Casse,[54] M. Cattaneo,[42] G. Cavallero,[55,42] V. Cavallini,[21,d] S. Celani,[43] J. Cerasoli,[10] D. Cervenkov,[57] A. J. Chadwick,[54] I. Chahrour,[78] M. G. Chapman,[48] M. Charles,[13] Ph. Charpentier,[42] C. A. Chavez Barajas,[54] M. Chefdeville,[8] C. Chen,[3] S. Chen,[4] A. Chernov,[35] S. Chernyshenko,[46] V. Chobanova,[40] S. Cholak,[43] M. Chrzaszcz,[35] A. Chubykin,[38] V. Chulikov,[38] P. Ciambrone,[23] M. F. Cicala,[50] X. Cid Vidal,[40] G. Ciezarek,[42] P. Cifra,[42] G. Ciullo,[21,d] P. E. L. Clarke,[52] M. Clemencic,[42] H. V. Cliff,[49] J. Closier,[42] J. L. Cobbledick,[56] V. Coco,[42] J. A. B. Coelho,[11] J. Cogan,[10] E. Cogneras,[9] L. Cojocariu,[37] P. Collins,[42] T. Colombo,[42] L. Congedo,[19] A. Contu,[27] N. Cooke,[47] I. Corredoira,[40] G. Corti,[42] B. Couturier,[42] D. C. Craik,[44] M. Cruz Torres,[1,h] R. Currie,[52] C. L. Da Silva,[61] S. Dadabaev,[38] L. Dai,[65] X. Dai,[5] E. Dall'Occo,[15] J. Dalseno,[40] C. D'Ambrosio,[42] J. Daniel,[9] A. Danilina,[38] P. d'Argent,[19] J. E. Davies,[56] A. Davis,[56] O. De Aguiar Francisco,[56] J. de Boer,[42] K. De Bruyn,[73] S. De Capua,[56] M. De Cian,[43] U. De Freitas Carneiro Da Graca,[1] E. De Lucia,[23] J. M. De Miranda,[1] L. De Paula,[2] M. De Serio,[19,i] D. De Simone,[44] P. De Simone,[23] F. De Vellis,[15] J. A. de Vries,[74] C. T. Dean,[61] F. Debernardis,[19,i] D. Decamp,[8] V. Dedu,[10] L. Del Buono,[13] B. Delaney,[58] H.-P. Dembinski,[15] V. Denysenko,[44] O. Deschamps,[9] F. Dettori,[27,j] B. Dey,[71] P. Di Nezza,[23] I. Diachkov,[38] S. Didenko,[38] L. Dieste Maronas,[40] S. Ding,[62] V. Dobishuk,[46] A. Dolmatov,[38] C. Dong,[3] A. M. Donohoe,[18] F. Dordei,[27] A. C. dos Reis,[1] L. Douglas,[53] A. G. Downes,[8] P. Duda,[75] M. W. Dudek,[35] L. Dufour,[42] V. Duk,[72] P. Durante,[42] M. M. Duras,[75] J. M. Durham,[61] D. Dutta,[56] A. Dziurda,[35] A. Dzyuba,[38] S. Easo,[51] U. Egede,[63] V. Egorychev,[38] C. Eirea Orro,[40] S. Eisenhardt,[52] E. Ejopu,[56] S. Ek-In,[43] L. Eklund,[77] J. Ellbracht,[15] S. Ely,[55] A. Ene,[37] E. Epple,[59] S. Escher,[14] J. Eschle,[44] S. Esen,[44] T. Evans,[56] F. Fabiano,[27,j] L. N. Falcao,[1] Y. Fan,[6] B. Fang,[11,68] L. Fantini,[72,k] M. Faria,[43] S. Farry,[54] D. Fazzini,[26,e] L. F Felkowski,[75] M. Feo,[42] M. Fernandez Gomez,[40] A. D. Fernez,[60] F. Ferrari,[20] L. Ferreira Lopes,[43] F. Ferreira Rodrigues,[2] S. Ferreres Sole,[32] M. Ferrillo,[44] M. Ferro-Luzzi,[42] S. Filippov,[38] R. A. Fini,[19] M. Fiorini,[21,d] M. Firlej,[34] K. M. Fischer,[57] D. S. Fitzgerald,[78] C. Fitzpatrick,[56] T. Fiutowski,[34] F. Fleuret,[12] M. Fontana,[13] F. Fontanelli,[24,g] R. Forty,[42] D. Foulds-Holt,[49] V. Franco Lima,[54] M. Franco Sevilla,[60] M. Frank,[42] E. Franzoso,[21,d] G. Frau,[17] C. Frei,[42] D. A. Friday,[53] J. Fu,[6] Q. Fuehring,[15] T. Fulghesu,[13] E. Gabriel,[32] G. Galati,[19,i] M. D. Galati,[32] A. Gallas Torreira,[40] D. Galli,[20,f] S. Gambetta,[52,42] Y. Gan,[3] M. Gandelman,[2] P. Gandini,[25] Y. Gao,[7] Y. Gao,[5] M. Garau,[27,j] L. M. Garcia Martin,[50] P. Garcia Moreno,[39] J. García Pardiñas,[26,e] B. Garcia Plana,[40] F. A. Garcia Rosales,[12] L. Garrido,[39] C. Gaspar,[42] R. E. Geertsema,[32] D. Gerick,[17] L. L. Gerken,[15]

E. Gersabeck,[56] M. Gersabeck,[56] T. Gershon,[50] L. Giambastiani,[28] V. Gibson,[49] H. K. Giemza,[36] A. L. Gilman,[57] M. Giovannetti,[23,l] A. Gioventù,[40] P. Gironella Gironell,[39] C. Giugliano,[21,d] M. A. Giza,[35] K. Gizdov,[52] E. L. Gkougkousis,[42] V. V. Gligorov,[13,42] C. Göbel,[64] E. Golobardes,[76] D. Golubkov,[38] A. Golutvin,[55,38] A. Gomes,[1,m] S. Gomez Fernandez,[39] F. Goncalves Abrantes,[57] M. Goncerz,[35] G. Gong,[3] I. V. Gorelov,[38] C. Gotti,[26] J. P. Grabowski,[70] T. Grammatico,[13] L. A. Granado Cardoso,[42] E. Graugés,[39] E. Graverini,[43] G. Graziani, A. T. Grecu,[37] L. M. Greeven,[32] N. A. Grieser,[59] L. Grillo,[53] S. Gromov,[38] B. R. Gruberg Cazon,[57] C. Gu,[3] M. Guarise,[21,d] M. Guittiere,[11] P. A. Günther,[17] E. Gushchin,[38] A. Guth,[14] Y. Guz,[38] T. Gys,[42] T. Hadavizadeh,[63] C. Hadjivasiliou,[60] G. Haefeli,[43] C. Haen,[42] J. Haimberger,[42] S. C. Haines,[49] T. Halewood-leagas,[54] M. M. Halvorsen,[42] P. M. Hamilton,[60] J. Hammerich,[54] Q. Han,[7] X. Han,[17] E. B. Hansen,[56] S. Hansmann-Menzemer,[17] L. Hao,[6] N. Harnew,[57] T. Harrison,[54] C. Hasse,[42] M. Hatch,[42] J. He,[6,n] K. Heijhoff,[32] F. H Hemmer,[42] C. Henderson,[59] R. D. L. Henderson,[63,50] A. M. Hennequin,[58] K. Hennessy,[54] L. Henry,[42] J. Herd,[55] J. Heuel,[14] A. Hicheur,[2] D. Hill,[43] M. Hilton,[56] S. E. Hollitt,[15] J. Horswill,[56] R. Hou,[7] Y. Hou,[8] J. Hu,[17] J. Hu,[66] W. Hu,[5] X. Hu,[3] W. Huang,[6] X. Huang,[68] W. Hulsbergen,[32] R. J. Hunter,[50] M. Hushchyn,[38] D. Hutchcroft,[54] P. Ibis,[15] M. Idzik,[34] D. Ilin,[38] P. Ilten,[59] A. Inglessi,[38] A. Iniukhin,[38] A. Ishteev,[38] K. Ivshin,[38] R. Jacobsson,[42] H. Jage,[14] S. J. Jaimes Elles,[41] S. Jakobsen,[42] E. Jans,[32] B. K. Jashal,[41] A. Jawahery,[60] V. Jevtic,[15] E. Jiang,[60] X. Jiang,[4,6] Y. Jiang,[6] M. John,[57] D. Johnson,[58] C. R. Jones,[49] T. P. Jones,[50] B. Jost,[42] N. Jurik,[42] I. Juszczak,[35] S. Kandybei,[45] Y. Kang,[3] M. Karacson,[42] D. Karpenkov,[38] M. Karpov,[38] J. W. Kautz,[59] F. Keizer,[42] D. M. Keller,[62] M. Kenzie,[50] T. Ketel,[32] B. Khanji,[15] A. Kharisova,[38] S. Kholodenko,[38] G. Khreich,[11] T. Kirn,[14] V. S. Kirsebom,[43] O. Kitouni,[58] S. Klaver,[33] N. Kleijne,[29,c] K. Klimaszewski,[36] M. R. Kmiec,[36] S. Koliiev,[46] L. Kolk,[15] A. Kondybayeva,[38] A. Konoplyannikov,[38] P. Kopciewicz,[34] R. Kopecna,[17] P. Koppenburg,[32] M. Korolev,[38] I. Kostiuk,[32,46] O. Kot,[46] S. Kotriakhova, A. Kozachuk,[38] P. Kravchenko,[38] L. Kravchuk,[38] R. D. Krawczyk,[42] M. Kreps,[50] S. Kretzschmar,[14] P. Krokovny,[38] W. Krupa,[34] W. Krzemien,[36] J. Kubat,[17] S. Kubis,[75] W. Kucewicz,[35] M. Kucharczyk,[35] V. Kudryavtsev,[38] E. K Kulikova,[38] A. Kupsc,[77] D. Lacarrere,[42] G. Lafferty,[56] A. Lai,[27] A. Lampis,[27,j] D. Lancierini,[44] C. Landesa Gomez,[40] J. J. Lane,[56] R. Lane,[48] C. Langenbruch,[14] J. Langer,[15] O. Lantwin,[38] T. Latham,[50] F. Lazzari,[29,o] M. Lazzaroni,[25,p] R. Le Gac,[10] S. H. Lee,[78] R. Lefèvre,[9] A. Leflat,[38] S. Legotin,[38] P. Lenisa,[21,d] O. Leroy,[10] T. Lesiak,[35] B. Leverington,[17] A. Li,[3] H. Li,[66] K. Li,[7] P. Li,[17] P.-R. Li,[67] S. Li,[7] T. Li,[4] T. Li,[66] Y. Li,[4] Z. Li,[62] X. Liang,[62] C. Lin,[6] T. Lin,[51] R. Lindner,[42] V. Lisovskyi,[15] R. Litvinov,[27,j] G. Liu,[66] H. Liu,[6] Q. Liu,[6] S. Liu,[4,6] A. Lobo Salvia,[39] A. Loi,[27] R. Lollini,[72] J. Lomba Castro,[40] I. Longstaff,[53] J. H. Lopes,[2] A. Lopez Huertas,[39] S. López Soliño,[40] G. H. Lovell,[49] Y. Lu,[4,q] C. Lucarelli,[22,b] D. Lucchesi,[28,r] S. Luchuk,[38] M. Lucio Martinez,[74] V. Lukashenko,[32,46] Y. Luo,[3] A. Lupato,[56] E. Luppi,[21,d] A. Lusiani,[29,c] K. Lynch,[18] X.-R. Lyu,[6] R. Ma,[6] S. Maccolini,[15] F. Machefert,[11] F. Maciuc,[37] I. Mackay,[57] V. Macko,[43] L. R. Madhan Mohan,[48] A. Maevskiy,[38] D. Maisuzenko,[38] M. W. Majewski,[34] J. J. Malczewski,[35] S. Malde,[57] B. Malecki,[35,42] A. Malinin,[38] T. Maltsev,[38] G. Manca,[27,j] G. Mancinelli,[10] C. Mancuso,[11,25,p] R. Manera Escalero,[39] D. Manuzzi,[20] C. A. Manzari,[44] D. Marangotto,[25,p] J. F. Marchand,[8] U. Marconi,[20] S. Mariani,[22,b] C. Marin Benito,[39,42] J. Marks,[17] A. M. Marshall,[48] P. J. Marshall,[54] G. Martelli,[72,k] G. Martellotti,[30] L. Martinazzoli,[42,e] M. Martinelli,[26,e] D. Martinez Santos,[40] F. Martinez Vidal,[41] A. Massafferri,[1] M. Materok,[14] R. Matev,[42] A. Mathad,[44] V. Matiunin,[38] C. Matteuzzi,[26] K. R. Mattioli,[12] A. Mauri,[32] E. Maurice,[12] J. Mauricio,[39] M. Mazurek,[42] M. McCann,[55] L. Mcconnell,[18] T. H. McGrath,[56] N. T. McHugh,[53] A. McNab,[56] R. McNulty,[18] J. V. Mead,[54] B. Meadows,[59] G. Meier,[15] D. Melnychuk,[36] S. Meloni,[26,e] M. Merk,[32,74] A. Merli,[25,p] L. Meyer Garcia,[2] D. Miao,[4,6] M. Mikhasenko,[70,s] D. A. Milanes,[69] E. Millard,[50] M. Milovanovic,[42] M.-N. Minard,[8,a] A. Minotti,[26,e] T. Miralles,[9] S. E. Mitchell,[52] B. Mitreska,[15] D. S. Mitzel,[15] A. Mödden,[15] R. A. Mohammed,[57] R. D. Moise,[14] S. Mokhnenko,[38] T. Mombächer,[40] M. Monk,[50,63] I. A. Monroy,[69] S. Monteil,[9] A. Morcillo Gomez,[40] G. Morello,[23] M. J. Morello,[29,c] J. Moron,[34] A. B. Morris,[42] A. G. Morris,[50] R. Mountain,[62] H. Mu,[3] E. Muhammad,[50] F. Muheim,[52] M. Mulder,[73] K. Müller,[44] C. H. Murphy,[57] D. Murray,[56] R. Murta,[55] P. Muzzetto,[27,j] P. Naik,[48] T. Nakada,[43] R. Nandakumar,[51] T. Nanut,[42] I. Nasteva,[2] M. Needham,[52] N. Neri,[25,p] S. Neubert,[70] N. Neufeld,[42] P. Neustroev,[38] R. Newcombe,[55] J. Nicolini,[15,11] D. Nicotra,[74] E. M. Niel,[43] S. Nieswand,[14] N. Nikitin,[38] N. S. Nolte,[58] C. Normand,[8,27,j] J. Novoa Fernandez,[40] G. N Nowak,[59] C. Nunez,[78]

A. Oblakowska-Mucha,[34] V. Obraztsov,[38] T. Oeser,[14] D. P. O'Hanlon,[48] S. Okamura,[21,d] R. Oldeman,[27,j] F. Oliva,[52] C. J. G. Onderwater,[73] R. H. O'Neil,[52] J. M. Otalora Goicochea,[2] T. Ovsiannikova,[38] P. Owen,[44] A. Oyanguren,[41] O. Ozcelik,[52] K. O. Padeken,[70] B. Pagare,[50] P. R. Pais,[42] T. Pajero,[57] A. Palano,[19] M. Palutan,[23] Y. Pan,[56] G. Panshin,[38] L. Paolucci,[50] A. Papanestis,[51] M. Pappagallo,[19,i] L. L. Pappalardo,[21,d] C. Pappenheimer,[59] W. Parker,[60] C. Parkes,[56] B. Passalacqua,[21,d] G. Passaleva,[22] A. Pastore,[19] M. Patel,[55] C. Patrignani,[20,f] C. J. Pawley,[74] A. Pellegrino,[32] M. Pepe Altarelli,[42] S. Perazzini,[20] D. Pereima,[38] A. Pereiro Castro,[40] P. Perret,[9] K. Petridis,[48] A. Petrolini,[24,g] A. Petrov,[38] S. Petrucci,[52] M. Petruzzo,[25] H. Pham,[62] A. Philippov,[38] R. Piandani,[6] L. Pica,[29,c] M. Piccini,[72] B. Pietrzyk,[8] G. Pietrzyk,[11] M. Pili,[57] D. Pinci,[30] F. Pisani,[42] M. Pizzichemi,[26,42,e] V. Placinta,[37] J. Plews,[47] M. Plo Casasus,[40] F. Polci,[13,42] M. Poli Lener,[23] A. Poluektov,[10] N. Polukhina,[38] I. Polyakov,[42] E. Polycarpo,[2] S. Ponce,[42] D. Popov,[6,42] S. Popov,[38] S. Poslavskii,[38] K. Prasanth,[35] L. Promberger,[17] C. Prouve,[40] V. Pugatch,[46] V. Puill,[11] G. Punzi,[29,o] H. R. Qi,[3] W. Qian,[6] N. Qin,[3] S. Qu,[3] R. Quagliani,[43] N. V. Raab,[18] B. Rachwal,[34] J. H. Rademacker,[48] R. Rajagopalan,[62] M. Rama,[29] M. Ramos Pernas,[50] M. S. Rangel,[2] F. Ratnikov,[38] G. Raven,[33,42] M. Rebollo De Miguel,[41] F. Redi,[42] J. Reich,[48] F. Reiss,[56] C. Remon Alepuz,[41] Z. Ren,[3] P. K. Resmi,[10] R. Ribatti,[29,c] A. M. Ricci,[27] S. Ricciardi,[51] K. Richardson,[58] M. Richardson-Slipper,[52] K. Rinnert,[54] P. Robbe,[11] G. Robertson,[52] A. B. Rodrigues,[43] E. Rodrigues,[54] E. Rodriguez Fernandez,[40] J. A. Rodriguez Lopez,[69] E. Rodriguez Rodriguez,[40] D. L. Rolf,[42] A. Rollings,[57] P. Roloff,[42] V. Romanovskiy,[38] M. Romero Lamas,[40] A. Romero Vidal,[40] J. D. Roth,[78,a] M. Rotondo,[23] M. S. Rudolph,[62] T. Ruf,[42] R. A. Ruiz Fernandez,[40] J. Ruiz Vidal,[41] A. Ryzhikov,[38] J. Ryzka,[34] J. J. Saborido Silva,[40] N. Sagidova,[38] N. Sahoo,[47] B. Saitta,[27,j] M. Salomoni,[42] C. Sanchez Gras,[32] I. Sanderswood,[41] R. Santacesaria,[30] C. Santamarina Rios,[40] M. Santimaria,[23] E. Santovetti,[31,l] D. Saranin,[38] G. Sarpis,[14] M. Sarpis,[70] A. Sarti,[30] C. Satriano,[30,t] A. Satta,[31] M. Saur,[15] D. Savrina,[38] H. Sazak,[9] L. G. Scantlebury Smead,[57] A. Scarabotto,[13] S. Schael,[14] S. Scherl,[54] M. Schiller,[53] H. Schindler,[42] M. Schmelling,[16] B. Schmidt,[42] S. Schmitt,[14] O. Schneider,[43] A. Schopper,[42] M. Schubiger,[32] S. Schulte,[43] M. H. Schune,[11] R. Schwemmer,[42] B. Sciascia,[23] A. Sciuccati,[42] S. Sellam,[40] A. Semennikov,[38] M. Senghi Soares,[33] A. Sergi,[24,g] N. Serra,[44] L. Sestini,[28] A. Seuthe,[15] Y. Shang,[5] D. M. Shangase,[78] M. Shapkin,[38] I. Shchemerov,[38] L. Shchutska,[43] T. Shears,[54] L. Shekhtman,[38] Z. Shen,[5] S. Sheng,[4,6] V. Shevchenko,[38] B. Shi,[6] E. B. Shields,[26,e] Y. Shimizu,[11] E. Shmanin,[38] R. Shorkin,[38] J. D. Shupperd,[62] B. G. Siddi,[21,d] R. Silva Coutinho,[62] G. Simi,[28] S. Simone,[19,i] M. Singla,[63] N. Skidmore,[56] R. Skuza,[17] T. Skwarnicki,[62] M. W. Slater,[47] J. C. Smallwood,[57] J. G. Smeaton,[49] E. Smith,[44] K. Smith,[61] M. Smith,[55] A. Snoch,[32] L. Soares Lavra,[9] M. D. Sokoloff,[59] F. J. P. Soler,[53] A. Solomin,[38,48] A. Solovev,[38] I. Solovyev,[38] R. Song,[63] F. L. Souza De Almeida,[2] B. Souza De Paula,[2] B. Spaan,[15,a] E. Spadaro Norella,[25,p] E. Spedicato,[20] E. Spiridenkov,[38] P. Spradlin,[53] V. Sriskaran,[42] F. Stagni,[42] M. Stahl,[42] S. Stahl,[42] S. Stanislaus,[57] E. N. Stein,[42] O. Steinkamp,[44] O. Stenyakin,[38] H. Stevens,[15] S. Stone,[62,a] D. Strekalina,[38] Y. S Su,[6] F. Suljik,[57] J. Sun,[27] L. Sun,[68] Y. Sun,[60] P. Svihra,[56] P. N. Swallow,[47] K. Swientek,[34] A. Szabelski,[36] T. Szumlak,[34] M. Szymanski,[42] Y. Tan,[3] S. Taneja,[56] M. D. Tat,[57] A. Terentev,[38] F. Teubert,[42] E. Thomas,[42] D. J. D. Thompson,[47] K. A. Thomson,[54] H. Tilquin,[55] V. Tisserand,[9] S. T'Jampens,[8] M. Tobin,[4] L. Tomassetti,[21,d] G. Tonani,[25,p] X. Tong,[5] D. Torres Machado,[1] D. Y. Tou,[3] S. M. Trilov,[48] C. Trippl,[43] G. Tuci,[6] A. Tully,[43] N. Tuning,[32] A. Ukleja,[36] D. J. Unverzagt,[17] A. Usachov,[33] A. Ustyuzhanin,[38] U. Uwer,[17] A. Vagner,[38] V. Vagnoni,[20] A. Valassi,[42] G. Valenti,[20] N. Valls Canudas,[76] M. Van Dijk,[43] H. Van Hecke,[61] E. van Herwijnen,[55] C. B. Van Hulse,[40,u] M. van Veghel,[73] R. Vazquez Gomez,[39] P. Vazquez Regueiro,[40] C. Vázquez Sierra,[42] S. Vecchi,[21] J. J. Velthuis,[48] M. Veltri,[22,v] A. Venkateswaran,[43] M. Veronesi,[32] M. Vesterinen,[50] D. Vieira,[59] M. Vieites Diaz,[43] X. Vilasis-Cardona,[76] E. Vilella Figueras,[54] A. Villa,[20] P. Vincent,[13] F. C. Volle,[11] D. vom Bruch,[10] A. Vorobyev,[38] V. Vorobyev,[38] N. Voropaev,[38] K. Vos,[74] C. Vrahas,[52] J. Walsh,[29] G. Wan,[5] C. Wang,[17] G. Wang,[7] J. Wang,[5] J. Wang,[4] J. Wang,[3] J. Wang,[68] M. Wang,[25] R. Wang,[48] X. Wang,[66] Y. Wang,[7] Z. Wang,[44] Z. Wang,[3] Z. Wang,[6] J. A. Ward,[50,63] N. K. Watson,[47] D. Websdale,[55] Y. Wei,[5] B. D. C. Westhenry,[48] D. J. White,[56] M. Whitehead,[53] A. R. Wiederhold,[50] D. Wiedner,[15] G. Wilkinson,[57] M. K. Wilkinson,[59] I. Williams,[49] M. Williams,[58] M. R. J. Williams,[52] R. Williams,[49] F. F. Wilson,[51] W. Wislicki,[36] M. Witek,[35] L. Witola,[17] C. P. Wong,[61] G. Wormser,[11] S. A. Wotton,[49] H. Wu,[62] J. Wu,[7] K. Wyllie,[42] Z. Xiang,[6] D. Xiao,[7] Y. Xie,[7] A. Xu,[5] J. Xu,[6]

L. Xu,[3] L. Xu,[3] M. Xu,[50] Q. Xu,[6] Z. Xu,[9] Z. Xu,[6] D. Yang,[3] S. Yang,[6] X. Yang,[5] Y. Yang,[6] Z. Yang,[5] Z. Yang,[60] L. E. Yeomans,[54] V. Yeroshenko,[11] H. Yeung,[56] H. Yin,[7] J. Yu,[65] X. Yuan,[62] E. Zaffaroni,[43] M. Zavertyaev,[16] M. Zdybal,[35] O. Zenaiev,[42] M. Zeng,[3] C. Zhang,[5] D. Zhang,[7] L. Zhang,[3] S. Zhang,[65] S. Zhang,[5] Y. Zhang,[5] Y. Zhang,[57] Y. Zhao,[17] A. Zharkova,[38] A. Zhelezov,[17] Y. Zheng,[6] T. Zhou,[5] X. Zhou,[6] Y. Zhou,[6] V. Zhovkovska,[11] X. Zhu,[3] X. Zhu,[7] Z. Zhu,[6] V. Zhukov,[14,38] Q. Zou,[4,6] S. Zucchelli,[20,f] D. Zuliani,[28] and G. Zunica[56]

(LHCb Collaboration)

[1]*Centro Brasileiro de Pesquisas Físicas (CBPF), Rio de Janeiro, Brazil*
[2]*Universidade Federal do Rio de Janeiro (UFRJ), Rio de Janeiro, Brazil*
[3]*Center for High Energy Physics, Tsinghua University, Beijing, China*
[4]*Institute of High Energy Physics (IHEP), Beijing, China*
[5]*School of Physics State Key Laboratory of Nuclear Physics and Technology, Peking University, Beijing, China*
[6]*University of Chinese Academy of Sciences, Beijing, China*
[7]*Institute of Particle Physics, Central China Normal University, Wuhan, Hubei, China*
[8]*Université Savoie Mont Blanc, CNRS, IN2P3-LAPP, Annecy, France*
[9]*Université Clermont Auvergne, CNRS/IN2P3, LPC, Clermont-Ferrand, France*
[10]*Aix Marseille Université, CNRS/IN2P3, CPPM, Marseille, France*
[11]*Université Paris-Saclay, CNRS/IN2P3, IJCLab, Orsay, France*
[12]*Laboratoire Leprince-Ringuet, CNRS/IN2P3, Ecole Polytechnique, Institut Polytechnique de Paris, Palaiseau, France*
[13]*LPNHE, Sorbonne Université, Paris Diderot Sorbonne Paris Cité, CNRS/IN2P3, Paris, France*
[14]*I. Physikalisches Institut, RWTH Aachen University, Aachen, Germany*
[15]*Fakultät Physik, Technische Universität Dortmund, Dortmund, Germany*
[16]*Max-Planck-Institut für Kernphysik (MPIK), Heidelberg, Germany*
[17]*Physikalisches Institut, Ruprecht-Karls-Universität Heidelberg, Heidelberg, Germany*
[18]*School of Physics, University College Dublin, Dublin, Ireland*
[19]*INFN Sezione di Bari, Bari, Italy*
[20]*INFN Sezione di Bologna, Bologna, Italy*
[21]*INFN Sezione di Ferrara, Ferrara, Italy*
[22]*INFN Sezione di Firenze, Firenze, Italy*
[23]*INFN Laboratori Nazionali di Frascati, Frascati, Italy*
[24]*INFN Sezione di Genova, Genova, Italy*
[25]*INFN Sezione di Milano, Milano, Italy*
[26]*INFN Sezione di Milano-Bicocca, Milano, Italy*
[27]*INFN Sezione di Cagliari, Monserrato, Italy*
[28]*Università degli Studi di Padova, Università e INFN, Padova, Italy*
[29]*INFN Sezione di Pisa, Pisa, Italy*
[30]*INFN Sezione di Roma La Sapienza, Roma, Italy*
[31]*INFN Sezione di Roma Tor Vergata, Roma, Italy*
[32]*Nikhef National Institute for Subatomic Physics, Amsterdam, Netherlands*
[33]*Nikhef National Institute for Subatomic Physics and VU University Amsterdam, Amsterdam, Netherlands*
[34]*AGH—University of Science and Technology, Faculty of Physics and Applied Computer Science, Kraków, Poland*
[35]*Henryk Niewodniczanski Institute of Nuclear Physics Polish Academy of Sciences, Kraków, Poland*
[36]*National Center for Nuclear Research (NCBJ), Warsaw, Poland*
[37]*Horia Hulubei National Institute of Physics and Nuclear Engineering, Bucharest-Magurele, Romania*
[38]*Affiliated with an institute covered by a cooperation agreement with CERN*
[39]*ICCUB, Universitat de Barcelona, Barcelona, Spain*
[40]*Instituto Galego de Física de Altas Enerxías (IGFAE), Universidade de Santiago de Compostela, Santiago de Compostela, Spain*
[41]*Instituto de Fisica Corpuscular, Centro Mixto Universidad de Valencia—CSIC, Valencia, Spain*
[42]*European Organization for Nuclear Research (CERN), Geneva, Switzerland*
[43]*Institute of Physics, Ecole Polytechnique Fédérale de Lausanne (EPFL), Lausanne, Switzerland*
[44]*Physik-Institut, Universität Zürich, Zürich, Switzerland*
[45]*NSC Kharkiv Institute of Physics and Technology (NSC KIPT), Kharkiv, Ukraine*

[46]Institute for Nuclear Research of the National Academy of Sciences (KINR), Kyiv, Ukraine
[47]University of Birmingham, Birmingham, United Kingdom
[48]H.H. Wills Physics Laboratory, University of Bristol, Bristol, United Kingdom
[49]Cavendish Laboratory, University of Cambridge, Cambridge, United Kingdom
[50]Department of Physics, University of Warwick, Coventry, United Kingdom
[51]STFC Rutherford Appleton Laboratory, Didcot, United Kingdom
[52]School of Physics and Astronomy, University of Edinburgh, Edinburgh, United Kingdom
[53]School of Physics and Astronomy, University of Glasgow, Glasgow, United Kingdom
[54]Oliver Lodge Laboratory, University of Liverpool, Liverpool, United Kingdom
[55]Imperial College London, London, United Kingdom
[56]Department of Physics and Astronomy, University of Manchester, Manchester, United Kingdom
[57]Department of Physics, University of Oxford, Oxford, United Kingdom
[58]Massachusetts Institute of Technology, Cambridge, Massachusetts, USA
[59]University of Cincinnati, Cincinnati, Ohio, USA
[60]University of Maryland, College Park, Maryland, USA
[61]Los Alamos National Laboratory (LANL), Los Alamos, New Mexico, USA
[62]Syracuse University, Syracuse, New York, USA
[63]School of Physics and Astronomy, Monash University, Melbourne, Australia (associated with Department of Physics, University of Warwick, Coventry, United Kingdom)
[64]Pontifícia Universidade Católica do Rio de Janeiro (PUC-Rio), Rio de Janeiro, Brazil (associated with Universidade Federal do Rio de Janeiro (UFRJ), Rio de Janeiro, Brazil)
[65]Physics and Micro Electronic College, Hunan University, Changsha City, China (associated with Institute of Particle Physics, Central China Normal University, Wuhan, Hubei, China)
[66]Guangdong Provincial Key Laboratory of Nuclear Science, Guangdong-Hong Kong Joint Laboratory of Quantum Matter, Institute of Quantum Matter, South China Normal University, Guangzhou, China (associated with Center for High Energy Physics, Tsinghua University, Beijing, China)
[67]Lanzhou University, Lanzhou, China (associated with Institute of High Energy Physics (IHEP), Beijing, China)
[68]School of Physics and Technology, Wuhan University, Wuhan, China (associated with Center for High Energy Physics, Tsinghua University, Beijing, China)
[69]Departamento de Fisica, Universidad Nacional de Colombia, Bogota, Colombia (associated with LPNHE, Sorbonne Université, Paris Diderot Sorbonne Paris Cité, CNRS/IN2P3, Paris, France)
[70]Universität Bonn—Helmholtz-Institut für Strahlen und Kernphysik, Bonn, Germany (associated with Physikalisches Institut, Ruprecht-Karls-Universität Heidelberg, Heidelberg, Germany)
[71]Eotvos Lorand University, Budapest, Hungary (associated with European Organization for Nuclear Research (CERN), Geneva, Switzerland)
[72]INFN Sezione di Perugia, Perugia, Italy (associated with INFN Sezione di Ferrara, Ferrara, Italy)
[73]Van Swinderen Institute, University of Groningen, Groningen, Netherlands (associated with Nikhef National Institute for Subatomic Physics, Amsterdam, Netherlands)
[74]Universiteit Maastricht, Maastricht, Netherlands (associated with Nikhef National Institute for Subatomic Physics, Amsterdam, Netherlands)
[75]Tadeusz Kosciuszko Cracow University of Technology, Cracow, Poland (associated with Henryk Niewodniczanski Institute of Nuclear Physics Polish Academy of Sciences, Kraków, Poland)
[76]DS4DS, La Salle, Universitat Ramon Llull, Barcelona, Spain (associated with ICCUB, Universitat de Barcelona, Barcelona, Spain)
[77]Department of Physics and Astronomy, Uppsala University, Uppsala, Sweden (associated with School of Physics and Astronomy, University of Glasgow, Glasgow, United Kingdom)
[78]University of Michigan, Ann Arbor, Michigan, USA (associated with Syracuse University, Syracuse, New York, USA)

[a]Deceased.
[b]Also at Università di Firenze, Firenze, Italy.
[c]Also at Scuola Normale Superiore, Pisa, Italy.
[d]Also at Università di Ferrara, Ferrara, Italy.
[e]Also at Università di Milano Bicocca, Milano, Italy.
[f]Also at Università di Bologna, Bologna, Italy.
[g]Also at Università di Genova, Genova, Italy.
[h]Also at Universidad Nacional Autónoma de Honduras, Tegucigalpa, Honduras.
[i]Also at Università di Bari, Bari, Italy.
[j]Also at Università di Cagliari, Cagliari, Italy.

[k]Also at Università di Perugia, Perugia, Italy.
[l]Also at Università di Roma Tor Vergata, Roma, Italy.
[m]Also at Universidade de Brasília, Brasília, Brazil.
[n]Also at Hangzhou Institute for Advanced Study, UCAS, Hangzhou, China.
[o]Also at Università di Pisa, Pisa, Italy.
[p]Also at Università degli Studi di Milano, Milano, Italy.
[q]Also at Central South University, Changsha, China.
[r]Also at Università di Padova, Padova, Italy.
[s]Also at Excellence Cluster ORIGINS, Munich, Germany.
[t]Also at Università della Basilicata, Potenza, Italy.
[u]Also at Universidad de Alcalá, Alcalá de Henares, Spain.
[v]Also at Università di Urbino, Urbino, Italy.